The Journal of Immunology

Cutting Edge: Differential Segregation of the Src Homology 2-Containing Protein Tyrosine Phosphatase-1 Within the Early NK Cell Immune Synapse Distinguishes Noncytolytic from Cytolytic Interactions

Yatin M. Vyas, Hina Maniar and Bo Dupont

J Immunol 2002; 168:3150-3154; ;
doi: 10.4049/jimmunol.168.7.3150
http://www.jimmunol.org/content/168/7/3150

The Journal of Immunology is published twice each month by
The American Association of Immunologists, Inc.,
1451 Rockville Pike, Suite 650, Rockville, MD 20852

Print ISSN: 0022-1767 Online ISSN: 1550-6606.

Cutting Edge: Differential Segregation of the Src Homology 2-Containing Protein Tyrosine Phosphatase-1 Within the Early NK Cell Immune Synapse Distinguishes Noncytolytic from Cytolytic Interactions[1]

Yatin M. Vyas, Hina Maniar, and Bo Dupont[2]

Inhibitory NK receptors with ligand specificity for MHC class I recruit Src homology 2-containing protein tyrosine phosphatase-1 (SHP-1) phosphatase and prevent autocytotoxicity. Activation of SHP-1 depends upon Src kinase-mediated tyrosine phosphorylation of the cytoplasmic domain of the inhibitory receptor. In this study we demonstrate, by quantitative temporal analysis, that talin, Lck, and SHP-1 are recruited to the synapse within 1 min in both cytolytic and noncytolytic conjugates. Polarization of talin and Lck rapidly disappears in the noncytolytic interactions but persists in cytolytic interactions, where protein kinase C-θ, Src homology 2 domain-containing leukocyte protein of 76 kDa, and lysosomes are recruited within 5 min. At 1 min SHP-1 clusters in the periphery of the cytolytic synapse, whereas it clusters in the center of the noncytolytic synapse. Lck has multifocal distribution in both synapses consistent with the shared requirement for early tyrosine phosphorylation. Our studies indicate that the spatial location of SHP-1 in the synapse distinguishes noncytolytic from cytolytic interactions within the first minute. *The Journal of Immunology,* **2002, 168: 3150–3154.**

Natural killer cells are cytotoxic lymphocytes capable of destroying MHC class I-deficient target cells (1). Major regulatory control of cytolytic NK cell function is mediated by MHC class I molecules with ligand specificity for inhibitory NK cell receptors (2). Inhibitory NK receptors contain in the cytoplasmic domains one or more immunoreceptor tyrosine-based inhibitory motif, and ligand binding induces recruitment of cytoplasmic phosphatase, Src homology 2-containing protein tyrosine phosphatase-1 (SHP-1),[3] to the tyrosine-phosphorylated immunoreceptor tyrosine-based inhibitory motifs (3, 4). SHP-1 mediated dephosphorylation may occur already at the level of the activating receptors (5). Conjugate formation by NK cells and T cells with its target cells is a process mediated by integrins and other adhesion molecules (6, 7). The cytolytic NK cell undergoes morphological changes leading to translocation of the microtubule-organizing center, secretory lysosomes, and talin to the contact area (i.e., synapse) (8), where talin accumulates at the contact, forming an outer ring, while the cytolytic granules become assembled in the talin-depleted center of the synapse (9, 10). Furthermore, in cytolytic NK cell conjugates lipid rafts become polarized to the contact area and this redistribution requires activation of Src and Syk kinases (11). The inhibitory NK receptors and their corresponding MHC class I ligands colocalize in the contact area between NK cells and target cells (12, 13), and the ligand binding, in addition to blocking raft polarization (14), may also down-regulate integrin function, leading to temporal shortening of contact between effector and target cells (15). While the topology of signal transduction molecules in the immune synapses has been described in the CD4 T-APC conjugates (9), CD8 CTL-target cell conjugates (10), and NK cell conjugates (16), the temporal progression of the signaling events occurring at the cell-cell interface during NK cell interactions with susceptible and nonsusceptible target cells has not been characterized. To determine these sequential events in the NK cell immune synapse (NKIS), we have performed a quantitative temporal analysis in single NK cells of the distribution of key elements involved in initiation or inhibition of cytolytic effector function during the first 10 min of conjugate formation. We demonstrate that the spatial distribution of SHP-1 in the "early" immune synapse provides the physical environment in the NK cell for interruption of activation signals during interactions with noncytolytic targets, while this phosphatase is displaced when cytolytic effector function has to proceed.

Materials and Methods

Cells

NK cell clones were generated and maintained from freshly isolated PBMC of healthy donors homozygous for HLA-Cw*0304 as previously described (16). Clones ($CD56^+CD16^+CD3^-GL183^+EB6^-DX9^-CD94^+$) that demonstrated lysis of the MHC class I-deficient 721.221 EBV-B lymphoblastoid cell line (BLCL) and 721.221-Cw*0401 (non-self) EBV-BLCL but

Immunology Program, Sloan-Kettering Institute for Cancer Research, Memorial Sloan-Kettering Cancer Center, New York, NY 10021

Received for publication December 3, 2001. Accepted for publication February 4, 2002.

The costs of publication of this article were defrayed in part by the payment of page charges. This article must therefore be hereby marked *advertisement* in accordance with 18 U.S.C. Section 1734 solely to indicate this fact.

[1] This work was supported by National Institutes of Health Grants CA 08748 and CA 23766.

[2] Address correspondence and reprint requests to Dr. Bo Dupont, Immunology Program, Sloan-Kettering Institute for Cancer Research, Memorial Sloan-Kettering Cancer Center, 1275 York Avenue, New York, NY 10021. E-mail address: b-dupont@ski.mskcc.org

[3] Abbreviations used in this paper: SHP-1, Src homology 2-containing protein tyrosine phosphatase-1; RE, relative enrichment; SMAC, supramolecular activation cluster; NKIS, NK cell immune synapse; PKC-θ, protein kinase C-θ; SLP-76, Src homology 2 domain-containing leukocyte protein of 76 kDa; BLCL, B lymphoblastoid cell line.

0022-1767/02/$02.00

protection of 721.221-Cw*0304 (self) EBV-BLCL were used for conjugate analysis as previously reported (16).

Antibodies

Primary. NK cells were phenotyped with anti-KIR3DL1 (DX9), anti-KIR2DL2/3, 2DS2/3 (GL183), anti-KIR2DL1/2DS1 (EB6), and anti-human CD94 mAbs, which were purchased from Immunotech (Marseilles, France). Mouse monoclonal and goat polyclonal anti-human talin were purchased from Chemicon International (Temecula, CA) and Santa Cruz Biotechnology (Santa Cruz, CA) respectively. Affinity-purified goat polyclonal anti-human protein kinase C-θ (PKC-θ), rabbit polyclonal anti-human SHP-1, and Lck were purchased from Santa Cruz Biotechnology. Sheep anti-human Src homology 2 domain-containing leukocyte protein of 76 kDa (SLP-76) was a gift from Dr. G. Koretzky (University of Pennsylvania, Philadelphia, PA). Mouse anti-human lysosome-associated membrane protein (H4A3) was obtained from the Developmental Studies Hybridoma Bank, Department of Biological Sciences, University of Iowa (Ames, IA). Cells were labeled with any three primary Ab combinations of mouse, rabbit, goat, or sheep.

Secondary. Affinity-purified second Abs and species-absorbed conjugates (FITC, Cy3, Cy5) for multiple labeling were purchased from Chemicon International. Appropriate final dilutions and controls of these affinity-purified primary and secondary Ab were done for each experiment (16).

Conjugation assay and immunofluorescent cell imaging

NK cell-target cell conjugates were formed, immunofluorescent labeled, and analyzed after fixing at 1, 5, and 10 min as previously described (16). To facilitate identification of the target cell in an NK cell-target cell conjugate the target cells were preincubated with CellTracker Blue CMAC (Molecular Probes, Eugene, OR). A digital imaging system (Intelligent Imaging Innovations, Denver, CO) with a Zeiss Axiovert 200 M inverted microscope and Xenon light source (Zeiss, New York, NY) was used. Images were obtained both in two-dimensions (*x*-*y*-axis) and three-dimensions (*x*-*z*-axis) (9) and analyzed using the masking and statistics capabilities of SlideBook software (Intelligent Imaging Innovations). Sixty to 70 serial optical sections of 0.2-μm thickness were acquired for each label. Data were deconvolved using constrained iterative (three-dimensional) deconvolution algorithm with SlideBook software. The contact areas (synapses) delineated by segmentation were acquired following volume renderings.

Statistical analysis of cell imaging data

Lysosomes and signaling molecules were considered polarized to the cell-cell contact when they were located in the proximal one-third area of NK cell in contact with the target (16). Talin was considered polarized when it clustered at the contact, as determined by the fluorescent intensity. Thirty to 50 conjugates were analyzed for each molecule and target combination for each time point. It is specifically mentioned in the figures when fewer than 30 conjugates were analyzed. The relative enrichment (RE), which is the fluorescence per unit volume at the contact site divided by the fluorescence per unit volume of the entire cell, was determined and is described in *Results and Discussion* as percentage of translocation (17). NK cell contact areas (measured as a percentage) were defined as the volume of NK cell in contact with the target cell divided by the total NK cell volume, multiplied by 100, as previously described (17). For quantitative enrichment analysis, 10 conjugates each with 721.221 or 721.221-Cw*0304 targets for each time point were randomly selected, their immune synapses (i.e., the projection in *z*-axis of 60–70 serial optical sections) were analyzed for enrichment of Lck and SHP-1, and 20 conjugates for each time point were analyzed for enrichment of talin. Wilcoxon nonparametric two-sample test was used to determine the *p* values comparing the statistical differences in the enrichment of a molecule.

Results and Discussion

Polarization of talin, lysosomes, Lck, SHP-1, PKC-θ, and SLP-76 to the cell-cell contact area was determined by two-dimensional analysis of conjugates at 1, 5, and 10 min (Figs. 1 and 2). Talin, Lck, and SHP-1 were polarized to the interface in a majority of both the cytolytic and noncytolytic conjugates at 1 min but continued to remain polarized only in the cytolytic conjugates when analyzed over the next 10 min (Figs. 1 and 2). Therefore, recruitment of talin, Lck, and SHP-1 to the contact areas is a common early event for both the cytolytic and noncytolytic interactions. In the cytolytic conjugates, PKC-θ and lysosomes (i.e., lytic granules) were not recruited to the contact area before 5 min, whereas SLP-76 was already polarized at 1 min in about half of these conjugates, suggesting rapid formation of the activation complex. (Fig. 2, *A* and *B*). Therefore, in cytolytic conjugates talin accumulation preceded granule polarization, similar to what is observed in CTL (10). PKC-θ, SLP-76, and lysosomes become polarized in the cytolytic conjugates by 5 min (Fig. 2*B*), suggesting rapid initiation of the target cell killing, similar to the time taken by CTL to induce target cell death (10).

Because our two-dimensional analysis of cytolytic and noncytolytic conjugates at 1 min demonstrated similar polarization of Lck and SHP-1, it was of interest to determine whether these molecules had similar segregation patterns in the NKIS. Therefore, three-dimensional analysis of NKIS was made at the same time points for talin, Lck, and SHP-1. This included quantifying RE (the

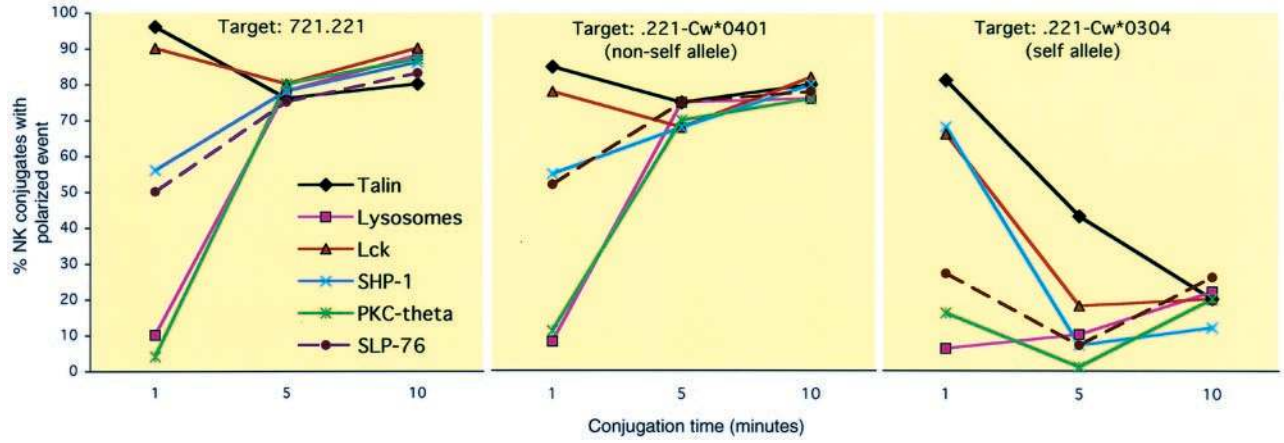

FIGURE 1. Temporal recruitment of molecules in cytolytic and noncytolytic conjugates. NK cell conjugates with 721.221 (*left panel*, susceptible target), .221-Cw*0401(*middle panel*, susceptible target), and .221-Cw*0304 (*right panel*, nonsusceptible target) were analyzed for indicated molecules (see symbols) at indicated time points (*x*-axis). Percentage of conjugates showing polarization of the indicated event to the cell-cell contact area, as analyzed in two dimensions, is shown (*y*-axis). The ranges of polarization for each component are given in detail in Fig. 2.

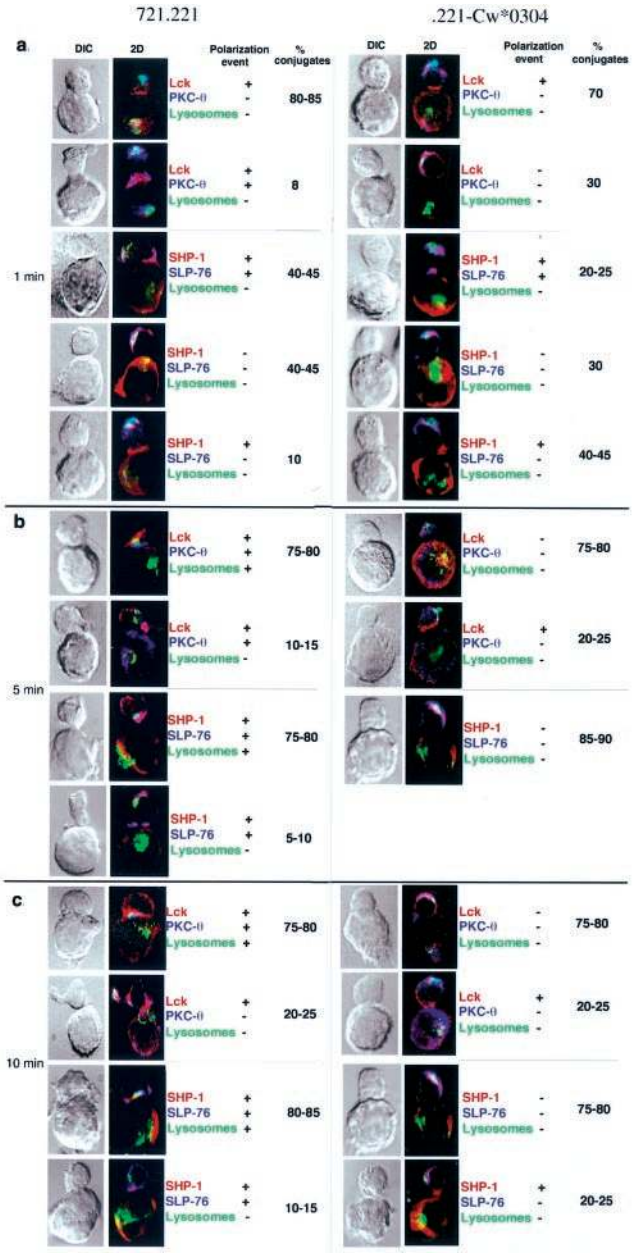

FIGURE 2. Two-dimensional temporal analysis of NK cell-target cell conjugates. NK cell conjugates with 721.221 (*left panel*, susceptible target) and .221-Cw*0304 (*right panel*, nonsusceptible target) were analyzed for indicated molecules (color-coded letters) at 1′ (*A*), 5′ (*B*), and 10′ (*C*). Conjugates are shown as Nomarski (differential interference contrast) and its corresponding two-dimensional fluorescent images. In each conjugate, NK cell is the top cell. For each target, the representative conjugates with different combinations of the polarized (+) or nonpolarized (−) molecules are shown along with the observed frequency (%) and range of the indicated event. A thin line separates each set of experiments. Any event occurring in < 5% of the conjugates is not shown. Overlapping distributions of labels results in yellow (red and green), pink (red and blue), and white (red, green, and blue) pseudo-colors.

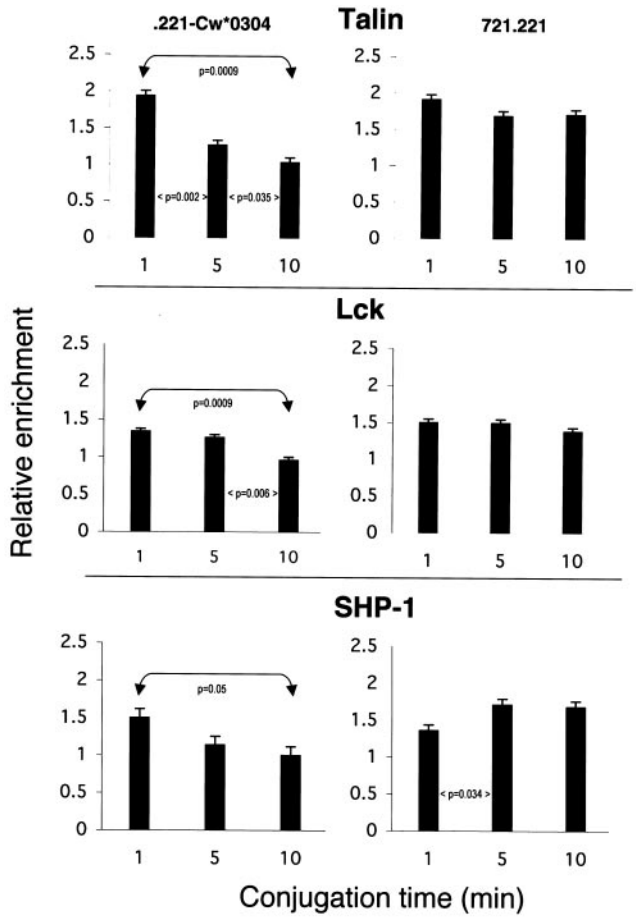

FIGURE 3. Translocation of NK cell talin, Lck, and SHP-1 in cytolytic and noncytolytic immune synapses analyzed from 1 to 10 min. The bar graph represents the mean (± SEM) values for the RE (*y*-axis) at the contact sites of the indicated molecules at indicated time points (*x*-axis). RE is described as the percentage of molecules within the NK cell that is translocated to the synapse, e.g., RE of 1.9 = 90% translocation and RE of 1 = baseline membrane distribution. NK cell conjugates with .221-Cw*0304 (*left panel*, nonsusceptible) and 721.221 (*right panel*, susceptible target) were imaged in 0.2-μm steps through the entire cell volume (10–15 μm). Data represent results obtained from 10–20 conjugates, each with 721.221 and .221-Cw*0304 for each time point. Two-sided *p* values were determined by Wilcoxon nonparametric two-sample test.

translocated fraction) (17) (Fig. 3) and visualizing the molecular distribution in the NKIS (Fig. 4).

In both the cytolytic and noncytolytic NKIS analyzed at 1 min, talin, Lck, and SHP-1 were greatly enriched above the baseline. Approximately 90% (RE = 1.9) of talin within the NK cell was translocated to both the cytolytic and noncytolytic NKIS at 1 min. However, the enrichment of talin, Lck, and SHP-1 rapidly decreased and reached baseline (RE = 1) distribution at 10 min in the noncytolytic interactions (Fig. 3). The early talin enrichment is probably mediated by Src kinase activation of integrins such as LFA-1 via the cytoplasmic domain of its β2 chain (18). In cytolytic conjugates enrichment of talin was sustained during the first 10 min, consistent with the ongoing tyrosine phosphorylation-dependent signaling. In contrast, talin enrichment was rapidly dissolved in noncytolytic conjugates, probably mediated by early interruption of tyrosine phosphorylation, which parallels the exclusion of the Src kinase, Lck, from the synaptic region during the ensuing 5–10 min (Figs. 1, 2, *B* and *C*, and 3). Similarly, the NK cell contact area in noncytolytic conjugates decreased from 13% at 1 min to 8% at 10 min ($p = 0.03$), suggesting the beginning of the deconjugation process. In contrast, the contact area in the cytolytic conjugates was 20% at 1 min and 17% at 10 min ($p = 0.5$), demonstrating sustained interaction during this period.

The spatio-temporal distribution of Lck, SHP-1, and talin in the NKIS was also determined at 1, 5, and 10 min (Fig. 4). This analysis demonstrates that the spatial distribution of SHP-1 within the

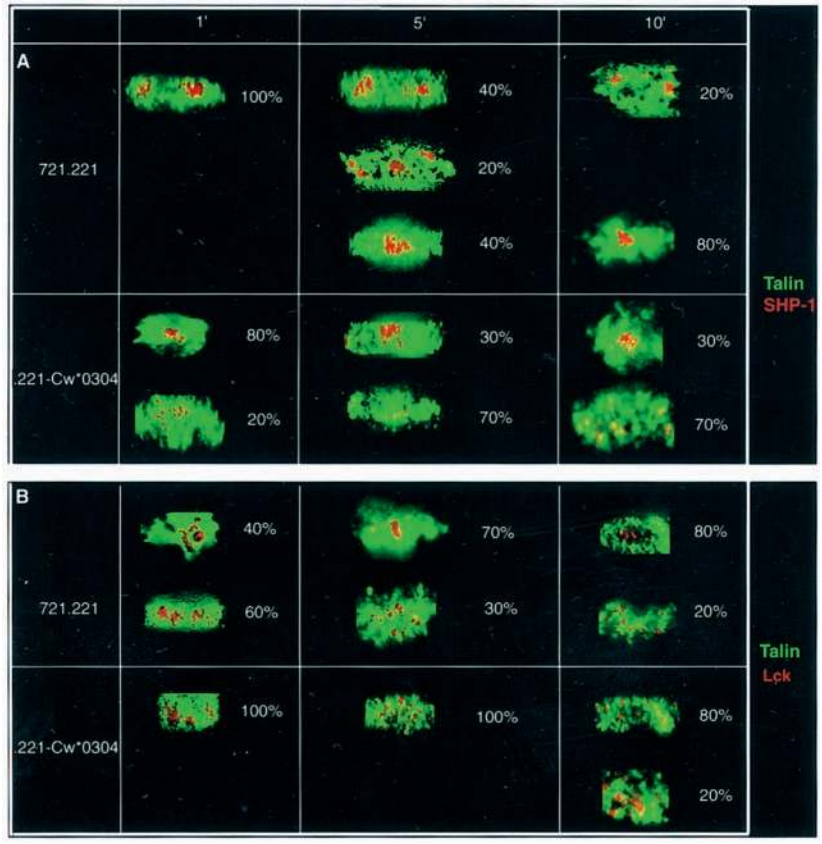

FIGURE 4. Three-dimensional temporal analysis of talin, Lck, and SHP-1 in cytolytic and noncytolytic NKIS. Synapses visualized as projection in *x*-*z*-axis of the NK cell conjugates with 721.221 (susceptible target) and .221-Cw*0304 (nonsusceptible target) labeled for talin (*A* and *B*, green), SHP-1 (*A*, red), and Lck (*B*, red) analyzed at 1′, 5′, and 10′ are shown. Representative NKIS with each target at the indicated time points are shown along with the frequency of the observed event (%). Data represent 20–30 immune synapses analyzed for each combination of the molecules from two independent experiments.

NKIS at 1 min clearly distinguishes the cytolytic from noncytolytic interactions at this early time (Fig. 4*A*). The cytolytic NKIS at 1 min displayed segregation of SHP-1 in the periphery (i.e., peripheral supramolecular activation cluster (peripheral SMAC)) (9) as two separate clusters each surrounded by talin. In contrast, the noncytolytic NKIS at 1 min displayed SHP-1 as a single cluster in the center (i.e., central supramolecular inhibition cluster) (19) surrounded by talin (Fig. 4*A*). This would suggest that SHP-1 in the noncytolytic interaction becomes localized in the vicinity of activating receptors and early mediators of activation signals such as SLP-76, linker for activation of T cells and ζ chain-associated protein 70, leading to interruption of signal transduction (5, 20, 21). Our findings of SHP-1 enrichment at the point of cell-cell contact complements previous studies in which the inhibitory NK receptors were shown to accumulate at this site (12, 13). Presumably the inhibitory killer Ig-like receptors, which recruit SHP-1, would also be located in the center of the "early" evolving synapse; however, a previous study demonstrated localization of inhibitory killer Ig-like receptors in the periphery of the "late" mature synapse (12). These issues require further studies with directly tagged receptor constructs. Interestingly, the segregation pattern for SHP-1 at 10 min in the cytolytic NKIS demonstrated clustering in the center (i.e., central SMAC), presumably recruited to the rafts in association with linker for activation of T cells as a component of the activation complex (22). Only 30% of the noncytolytic NKIS, at 10 min, showed SHP-1 clustered in the central supramolecular inhibition cluster, consistent with our previous observations (16) (Fig. 4*A*, 10′ column). In fact, 20–25% of 10-min noncytolytic conjugates also showed polarization of Lck (Fig. 2*C*) and quantitative enrichment of talin to the contact area (data not shown) similar to the 1-min conjugates, while the majority of these noncytolytic conjugates had baseline talin, Lck, and SHP-1 concentrations (RE = 1) in the NKIS (Fig. 3). This suggests completion of "self" recognition by the majority of primary conjugates by 10 min and formation of an early inhibitory NKIS by newly formed secondary conjugates.

The majority of cytolytic and noncytolytic NKIS had similar distribution of Lck at 1 min with formation of two to three scattered clusters enclosed by talin (Fig. 4*B*). At 5 and 10 min Lck clustered in the cSMAC in the majority of the cytolytic NKIS, whereas Lck remained dispersed as multiple small clusters in the majority of noncytolytic NKIS (Fig. 4*B*). The 5-min NKIS for talin, Lck, and SHP-1 displayed a spectrum of configurations varying from the typical patterns observed at 1 min to the predominant patterns seen at 10 min (Fig. 4, 5′ column). Furthermore, a minority of the 10-min NKIS displayed configurations similar to the 1-min NKIS, again suggesting formation of new secondary conjugates (Fig. 4, 10′ column). In cytolytic interactions recruitment of lysosomes to the contact area occurs within the first 5 min (Fig. 1). This is preceded by recruitment of SLP-76 and PKC-θ, which can be observed in some conjugates already at 1 min (Fig. 2*A*). It is likely that interactions between SLP-76 and SLP-76-associated phosphoprotein/Fyn-binding protein mediate the "inside-out" signaling, thereby sustaining adhesion during cytolytic interactions (23). The studies reported in this work show that NK cells form productive immune synapses with both the susceptible and nonsusceptible targets as early as 1 min into the interactions. Within these early synapses SHP-1 segregates into separate domains, allowing clear distinction between noncytolytic and cytolytic NKIS.

Acknowledgments

We thank the Ludwig Institute for Cancer Research (New York, NY) for access to digital fluorescence microscope with SlideBook software. We thank Dr. Lloyd J. Old for his encouragement and support.

References

1. Ljunggren, H. G., and K. Karre. 1990. In search of the "missing self": MHC molecules and NK cell recognition. *Immunol. Today 11:237.*
2. Lanier, L. L. 1998. NK cell receptors. *Annu. Rev. Immunol. 16:359.*
3. Burshtyn, D. N., A. M. Scharenberg, N. Wagtmann, S. Rajagopalan, K. Berrada, T. Yi, J. P. Kinet, and E. O. Long. 1996. Recruitment of tyrosine phosphatase HCP by the killer cell inhibitor receptor. *Immunity 4:77.*
4. Binstadt, B. A., K. M. Brumbaugh, C. J. Dick, A. M. Scharenberg, B. L. Williams, M. Colonna, L. L. Lanier, J. P. Kinet, R. T. Abraham, and P. J. Leibson. 1996. Sequential involvement of Lck and SHP-1 with MHC-recognizing receptors on NK cells inhibits FcR-initiated tyrosine kinase activation. *Immunity 5:629.*
5. Watzl, C., C. C. Stebbins, and E. O. Long. 2000. Cutting edge: NK cell inhibitory receptors prevent tyrosine phosphorylation of the activation receptor 2B4 (CD244). *J. Immunol. 165:3545.*
6. Wülfing, C., and M. M. Davis. 1998. A receptor/cytoskeletal movement triggered by costimulation during T cell activation. *Science 282:2266.*
7. Grakoui, A., S. K. Bromley, C. Sumen, M. M. Davis, A. S. Shaw, P. M. Allen, and M. L. Dustin. 1999. The immunological synapse: a molecular machine controlling T cell activation. *Science 285:221.*
8. Stinchcombe, J. C., and G. M. Griffiths. 2001. Normal and abnormal secretion by haemopoietic cells. *Immunology 103:10.*
9. Monks, C. R., B. A. Freiberg, H. Kupfer, N. Sciaky, and A. Kupfer. 1998. Three-dimensional segregation of supramolecular activation clusters in T cells. *Nature 395:82.*
10. Stinchcombe, J. C., G. Bossi, S. Booth, and G. M. Griffiths. 2001. The immunological synapse of CTL contains a secretory domain and membrane bridges. *Immunity 15:751.*
11. Lou, Z., D. Jevremovic, D. Billadeau, and P. Leibson. 2000. A balance between positive and negative signals in cytotoxic lymphocytes regulates the polarization of lipid rafts during the development of cell-mediated killing. *J. Exp. Med. 191:347.*
12. Davis, D. M., I. Chiu, M. Fassett, G. B. Cohen, O. Mandelboim, and J. L. Strominger. 1999. The human natural killer cell immune synapse. *Proc. Natl. Acad. Sci. USA 96:15062.*
13. Eriksson, M., J. C. Ryan, M. C. Nakamura, and C. L. Sentman. 1999. Ly49A inhibitory receptors redistribute on natural killer cells during target cell interaction. *Immunology 97:341.*
14. Fassett, M. S., D. M. Davis, M. M. Valter, G. B. Cohen, and J. L. Strominger. 2001. Signaling at the inhibitory natural killer cell immune synapse regulates lipid raft polarization but not class I MHC clustering. *Proc. Natl. Acad. Sci. USA 98:14547.*
15. Burshtyn, D. N., J. Shin, C. Stebbins, and E. O. Long. 2000. Adhesion to target cells is disrupted by the killer cell inhibitory receptor. *Curr. Biol. 10:777.*
16. Vyas, Y. M., K. M. Mehta, M. Morgan, H. Maniar, L. Butros, S. Jung, J. K. Burkhardt, and B. Dupont. 2001. Spatial organization of signal transduction molecules in the NK cell immune synapses during MHC class I-regulated noncytolytic and cytolytic interactions. *J. Immunol. 167:4358.*
17. Schaefer, B. C., M. F. Ware, P. Marrack, G. R. Fanger, J. W. Kappler, G. L. Johnson, and C. R. F. Monks. 1999. Live cell fluorescence imaging of T cell MEKK2: redistribution and activation in response to antigen stimulation of the T cell receptor. *Immunity 11:411.*
18. Calderwood, D. A., R. Zen, R. Grant, D. J. G. Rees, R. O. Hynes, and M. H. Ginsberg. 1999. The talin head domain binds to integrin β subunit cytoplasmic tails and regulates integrin activation. *J. Biol. Chem. 274:28071.*
19. Carlin, L. M., K. Eleme, F. E. McCann, and D. M. Davis. 2001. Intercellular transfer and supramolecular organization of human leukocyte antigen C at inhibitory natural killer cell immune synapses. *J. Exp. Med. 194:1507.*
20. Binstadt, B. A., D. D. Billadeau, D. Jevremovic, B. L. Williams, N. Fang, T. Yi, G. A. Koretzky, R. T. Abraham, and P. J. Leibson. 1998. SLP-76 is a direct substrate of SHP-1 recruited to killer cell inhibitory receptors. *J. Biol. Chem. 273:27518.*
21. Jevremovic, D., D. D. Billadeau, R. A. Schoon, C. J. Dick, B. J. Irvin, W. Zhang, L. E. Samelson, R. T. Abraham, and P. J. Leibson. 1999. Cutting edge: a role for the adaptor protein LAT in human NK cell-mediated cytotoxicity. *J. Immunol. 162:2453.*
22. Kosugi, A., J. Sakakura, K. Yasuda, M. Ogata, and T. Hamaoka. 2001. Involvement of SHP-1 tyrosine phosphatase in TCR-mediated signaling pathways in lipid rafts. *Immunity 14:669.*
23. Peterson, E. J., M. L. Woods, S. A. Dmowski, G. Derimanov, M. S. Jordan, J. N. Wu, P. S. Myung, Q.-H. Liu, J. T. Pribila, B. D. Freedman, et al. 2001. Coupling of the TCR to integrin activation by SLAP-130/Fyb. *Science 293:2263.*